Acoustic wave transparency for a multilayered sphere with acoustic metamaterials

Xiaoming Zhou and Gengkai Hu*

School of Science, Beijing Institute of Technology, Beijing 100081, People's Republic of China
(Received 9 November 2006; published 13 April 2007)

By analogy with the electromagnetic wave, the acoustic transparency phenomenon is analyzed for a multi-layered sphere with acoustic metamaterials. The neutral-inclusion concept is used to predict the transparency conditions in the quasistatic case, which are further confirmed by a full-wave analysis. The mechanism of the transparency is based on lowering the total-scattering cross section of the composite sphere. It is found that, to improve the transparency, the angle-dependent scattering cross section must also be minimized for all directions.

I. INTRODUCTION

The study of electromagnetic wave (EM) transparency induced by metamaterials has been intensified recently since the pioneer work by Alù and Engheta [1], who demonstrated how a small sphere could be made invisible. Since then, several papers [2–5] have been published to give more physical insights into this phenomenon. The theoretical investigations [2–4] revealed that invisibility could also be realized in the case of a wavelength much shorter than the particle size. In this situation, the refractive index of the designed devices will have to be position dependent. This introduces some difficulties for the physical realization of invisible devices. However, with the development of EM metamaterials [6], the transparency of an object whose dimension is larger than the operating wavelength can indeed be realized in experiment [7].

Recently, the analogy between left-handed EM metamaterial [8] and double-negative acoustic metamaterial has been identified [9]. Furthermore, it is found that sound waves can also be focused by a phononic crystal slab [10], similar to negative refraction by a photonic crystal [11]. So it is natural to ask whether the transparency can be achieved for acoustic waves by introducing acoustic metamaterials—i.e., materials with a negative modulus and/or negative density. In the static case, a negative modulus can be obtained for a tube structure in the post-buckling regime [12]. With decreasing force, the tube will have an increase in deformation. Recently, the negative modulus in the regime of an ultrasonic wave has been realized in a material with subwavelength sonic resonators [13], which can be considered as the acoustic analog of EM metamaterials. The double-negative acoustic metamaterial can be achieved in a composite of soft spheres suspended in a liquid [9], and the double negativity of the bulk modulus and density can occur in the same sonic frequency region in the presence of a monopolar-dipolar resonance.

In a previous paper [5], we have proposed the concept of "neutral inclusion" to investigate the transparency phenomenon for EM waves. A neutral inclusion is a simple pattern (coated sphere, etc.), which has been fully discussed by Mil-

ton [14]. When a neutral inclusion is embedded in a material made of assemblages of such patterns with gradual size (in order to fill the whole space), it will not perturb the outside fields. In this paper, we will use this idea to analyze the transparency phenomenon induced by acoustic metamaterials. For simplicity, we consider a multilayered sphere, in which all materials are considered as fluids or fluidlike materials; i.e., they do not support shear waves. We note that this assumption will not make the results of this paper useless, since most of the acoustic metamaterials reported recently are fluidlike materials [9,13].

II. THEORETICAL ANALYSIS

Figure 1 shows the cross section of a multilayered sphere, where the outer radius of the lth layer is r_l and each region ($l=1,2,\ldots,L+1$) is characterized by the bulk modulus κ_l, density ρ_l, and sound velocity $v_l=\sqrt{\kappa_l/\rho_l}$. The acoustic total-scattering cross section Q_s of the multilayered sphere can be computed in the framework of Mie theory [15], and it is expressed as
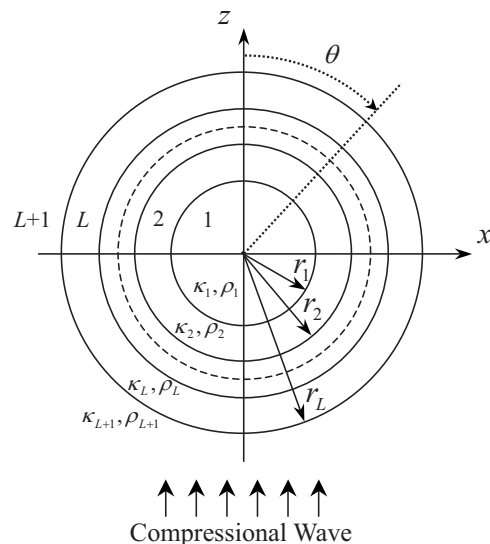

FIG. 1. Cross section of a multilayered sphere.

*Author to whom correspondence should be addressed. Electronic address: hugeng@bit.edu.cn

$$Q_s = \lambda_{L+1}^2 \sum_{n=0}^{\infty} \frac{|a_n|^2}{(2n+1)\pi}, \tag{1}$$

where λ_{L+1} is the wavelength in region $L+1$. The scattering coefficient $a_n = (2n+1)i^n A_n^{(L+1)}$ is calculated by using the equation

$$A_n^{(l+1)} = R_n(k_{l+1}r_l) \frac{v_{l+1}\rho_{l+1}H_n(k_l r_l) - v_l\rho_l D_n^{(1)}(k_{l+1}r_l)}{v_{l+1}\rho_{l+1}H_n(k_l r_l) - v_l\rho_l D_n^{(3)}(k_{l+1}r_l)}, \tag{2}$$

with

$$H_n(k_1 r_1) = D_n^{(1)}(k_1 r_1),$$

$$H_n(k_l r_l) = \frac{D_n^{(1)}(k_l r_l)R_n(k_l r_l) - A_n^{(l)}D_n^{(3)}(k_l r_l)}{R_n(k_l r_l) - A_n^{(l)}}, \quad l = 2,3,\ldots,L,$$

where $D_n^{(1)}(x) = j_n'(x)/j_n(x)$, $D_n^{(3)}(x) = h_n'(x)/h_n(x)$, and $R_n(x) = j_n(x)/h_n(x)$. $j_n(x)$ and $h_n(x)$ are the spherical Bessel function and spherical Hankel function of the first kind, respectively. The prime indicates the derivative with respect to x.

Using the above formulations, we can determine the quasistatic transparency condition by examining the first several scattering coefficients a_n. However, a more simple method is to utilize the "neutral-inclusion" concept [5,14]. The key point of this idea is to evaluate the effective bulk modulus and effective density of the multilayered sphere assemblage and let them be equal to those of the surrounding medium. In order to proceed, we will first discuss two simple cases—i.e., the equal-density case in which all densities are equal and the equal-modulus case in which all moduli are equal. Then we will examine the transparency phenomenon for acoustic waves in a general case.

A. Equal-density case

Consider firstly the case of a coated sphere ($L=2$). It is known that the effective bulk modulus κ_{eff} of the coated-sphere assemblage realizes the Hashin-Shtrikman (HS) bound [16]. When the shear moduli of the materials vanish, the effective bulk moduli will reduce to the Voigt bound—i.e.,

$$\kappa_{\text{eff}} = \frac{r_2^3 \kappa_1 \kappa_2}{r_1^3 \kappa_2 + (r_2^3 - r_1^3)\kappa_1}. \tag{3}$$

By letting $\kappa_{\text{eff}} = \kappa_3$, the transparency condition of a coated sphere can be obtained as

$$\frac{r_2^3}{\kappa_3} = \frac{r_1^3}{\kappa_1} + \frac{r_2^3 - r_1^3}{\kappa_2}. \tag{4}$$

It is noted that Eq. (4) can also be obtained when we examine the zeroth-order scattering coefficient a_0 in Eq. (1) and set it to zero in the small-particle approximation.

For EM waves, if the permittivity of one phase of the coated sphere is larger than that of the surrounding medium, the permittivity of the other one must be lower in order to satisfy the transparency condition [1,5]. However, for acoustic waves, we can find from Eq. (4) that if one bulk modulus

(for example, κ_1) of the coated sphere takes a negative value, the other one (κ_2) must be $0 < \kappa_2 < \kappa_3$. Both moduli can be lower than the modulus of the surrounding medium.

For the multilayered-sphere case, the effective bulk modulus of the assemblage made of the multilayered spheres can be derived based on the solution of a coated sphere, using the recursive method [5,14]. The recursive process is based on an assumption that the l-layer sphere can be considered as an effective core embedded in the lth-coating material. So the effective bulk modulus κ_{eff}^L of the multilayered-sphere assemblage can be determined by the equation

$$\frac{r_L^3}{\kappa_{\text{eff}}^L} = \frac{r_1^3}{\kappa_1} + \sum_{l=2}^{L} \frac{r_l^3 - r_{l-1}^3}{\kappa_l}. \tag{5}$$

With help of Eq. (5) and the neutral-inclusion concept, the quasistatic transparency condition for acoustic waves can be obtained by setting $\kappa_{\text{eff}}^L = \kappa_{L+1}$ if all the densities are equal.

B. Equal-modulus case

A region with different density from that of the surrounding can also scatter acoustic waves, as can be seen from Eq. (1). So there may exist transparency phenomena induced by densities. We still consider the multilayered-sphere configuration as discussed in the equal-density case, but by assuming that moduli of the materials are equal. Contrary to the equal-density case, the HS bound model cannot be applied for evaluating the effective density of the assemblage made of the multilayered spheres, since the density itself is not a transport quantity. For solid materials, the effective density will obey the mixture rule based on the mass conservation, while for a fluid matrix with inclusions, there may be an additional density due to the induced-mass effect [17]. For this case, the self-consistent method can be used to determine the effective density of the multilayered-sphere assemblage.

We first discuss a coated sphere and consider the case of long-wavelength limit where the single-scattering effect dominates. We embed a coated sphere in the effective medium made of the coated-sphere assemblage with the effective density ρ_{eff} and adjust the effective medium so that the total-scattering cross section of the coated sphere vanishes. With help of Eq. (1) and the equal-modulus assumption, the effective density ρ_{eff} of the coated-sphere assemblage can be estimated by

$$\rho_{\text{eff}} = \rho_2 + \frac{3f\rho_2(\rho_1 - \rho_2)}{3\rho_2 + 2(1-f)(\rho_1 - \rho_2)}, \tag{6}$$

where $f = r_1^3/r_2^3$. Equation (6) is the same as that obtained by using the Kuster-Toksöz method [17]. Using Eq. (6), the transparency condition of a coated sphere can be obtained by setting $\rho_{\text{eff}} = \rho_3$, leading to

$$\frac{(\rho_2 - \rho_3)(\rho_2 + 2\rho_1)}{(\rho_2 - \rho_1)(\rho_2 + 2\rho_3)} = \frac{r_1^3}{r_2^3}. \tag{7}$$

In the long-wavelength limit, Eq. (7) can also be obtained if we examine the first-order scattering coefficient a_1 of a

coated sphere and set it to be zero. The zeroth-order scattering coefficient a_0 always vanishes for this limit.

With Eq. (6) and the recursive method, the effective density of an l-layer sphere assemblage is given by

$$\rho_{\text{eff}}^l = \rho_l + \frac{3(1-f_l)\rho_l(\rho_{\text{eff}}^{l-1} - \rho_l)}{3\rho_l + 2f_l(\rho_{\text{eff}}^{l-1} - \rho_l)}, \quad l = 2, \dots, L, \quad (8)$$

where $f_l = 1 - r_{l-1}^3/r_l^3$ is the volume fraction of the lth layer in the l-layer sphere and $\rho_{\text{eff}}^1 = \rho_1$. Then in the quasistatic case, the corresponding transparency condition is given by $\rho_{\text{eff}}^L = \rho_{L+1}$ if all the bulk moduli of the multilayered sphere are equal. Especially for a doubly coated sphere ($L=3$), the transparency condition becomes

$$\frac{r_2^3(\rho_3 + 2\rho_4)}{r_3^3(\rho_3 - \rho_4)} = \frac{r_2^3(\rho_2 + 2\rho_1)(\rho_3 + 2\rho_2) + 2r_1^3(\rho_2 - \rho_1)(\rho_3 - \rho_2)}{r_2^3(\rho_2 + 2\rho_1)(\rho_3 - \rho_2) + r_1^3(\rho_2 - \rho_1)(\rho_2 + 2\rho_3)}.$$
$$(9)$$

C. General case

Now let us discuss the general case that each region of the system shown in Fig. 1 has not necessarily the same density or bulk modulus. For the coated-sphere configuration, the self-consistent method can be employed to predict the effective bulk modulus κ_{eff} and effective density ρ_{eff} of the coated-sphere assemblage. To do this, we embed a coated sphere in the effective medium made of the coated-sphere assemblage with κ_{eff} and ρ_{eff} and adjust the effective medium so that the total scattering cross section of the coated sphere vanishes. In the long-wavelength limit, it is interesting to find that Eq. (3) for effective bulk modulus κ_{eff} and Eq. (6) for effective density ρ_{eff} are recovered. With Eqs. (3) and (6), the transparency conditions for the coated sphere in the general case can be obtained by setting $\kappa_{\text{eff}} = \kappa_3$ and $\rho_{\text{eff}} = \rho_3$. So a coated sphere will be acoustically transparent when Eqs. (4) and (7) are satisfied simultaneously. It is noted that transparency conditions (4) and (7) can also be obtained when we let the numerator of scattering coefficients a_0 and a_1 of the coated sphere be equal to zero, respectively. For the multilayered-sphere configuration, the corresponding effective bulk modulus and effective density can be found in Eqs. (5) and (8) with help of the recursive method. So the transparency conditions in the quasistatic case can be obtained by setting $\kappa_{\text{eff}}^L = \kappa_{L+1}$ and $\rho_*^L = \rho_{L+1}$.

The above results show that the influences of the bulk modulus and density on the total scattering are actually uncoupled in the quasistatic case. So the discussions given previously on two special cases (i.e., equal-density case and equal-modulus case) are helpful for the investigation of transparency phenomenon in a general case. Although these analyses are given for the quasistatic case, they will be still useful for investigating the transparency phenomenon in the full-wave dynamic case. This will be verified in the following section.

III. NUMERICAL RESULTS AND DISCUSSIONS

In this section, we will perform numerical computations for the full-wave scattering case in order to check the quasi-
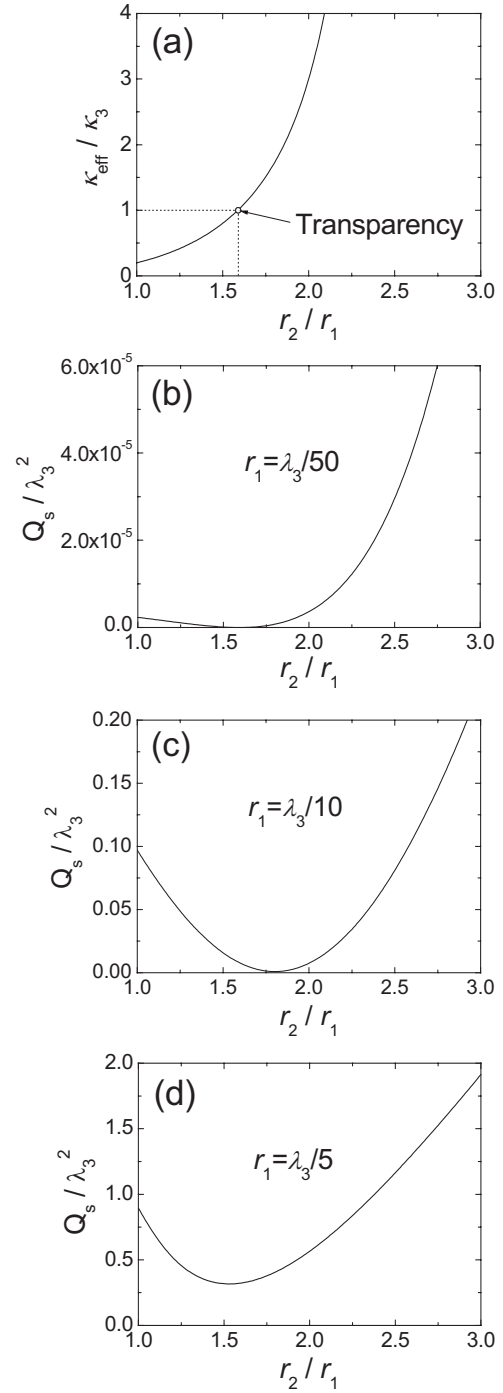

FIG. 2. (a) Normalized effective bulk modulus $\kappa_{\text{eff}}/\kappa_3$ of a coated-sphere assemblage calculated with Eq. (3) and normalized total-scattering cross section of the coated sphere with three different core radii (b) $r_1 = \lambda_3/50$, (c) $r_1 = \lambda_3/10$, and (d) $r_1 = \lambda_3/5$ as a function of ratio r_2/r_1 ($\kappa_1 = 0.2\kappa_3$, $\kappa_2 = -3\kappa_3$, and $\rho_1 = \rho_2 = \rho_3$).

static transparency conditions. First of all, it is necessary to give a study of the influence of particle size on the transparency, since the particle size plays a key role in the scattering of the multilayered sphere. Consider a coated sphere with material parameters $\kappa_1 = 0.2\kappa_3$, $\kappa_2 = -3\kappa_3$, and $\rho_1 = \rho_2 = \rho_3$. From Eq. (3), the computed effective bulk modulus $\kappa_{\text{eff}}/\kappa_3$ of the coated-sphere assemblage is shown in Fig. 2(a) as a

function of ratio r_2/r_1. It is expected that the transparency of the coated sphere will take place at about $r_2/r_1 = 1.6$, for which $\kappa_{\mathrm{eff}}/\kappa_3 \approx 1$. Figures 2(b), 2(c), and 2(d) show the normalized total-scattering cross section Q_s/λ_3^2 of coated spheres with the core radii $r_1 = \lambda_3/50$, $r_1 = \lambda_3/10$, and $r_1 = \lambda_3/5$, respectively. When the particle size is very small ($r_1 = \lambda_3/50$), the transparency of a coated sphere indeed occurs at around $r_2/r_1 = 1.6$, where Q_s/λ_3^2 is extremely low. When the core radius is increased to $r_1 = \lambda_3/10$, the ratio r_2/r_1 corresponding to the minimum scattering still exists, but has been shifted upwards. This shifting phenomenon can be attributed to the large particle effect, analogous to the case of electromagnetic waves. When the particle size is further increased ($r_1 = \lambda_3/5$), the coated sphere cannot be acoustically transparent any longer. The above results show that the transparency of a coated sphere is easily realized when the particle size is relatively small. Note that this result is not limited to coated spheres that satisfy the equal-density case. For this reason, we typically choose the core radius to be $r_1 = \lambda_3/20$ in the following computations and discuss how the quasistatic conditions can be used to predict the transparency phenomenon.

We again give an example of the equal-density case. Consider the parameters $\kappa_1 = 0.1\kappa_3$, $\kappa_2 = -2\kappa_3$, $\rho_1 = \rho_2 = \rho_3$, and $r_1 = \lambda_3/20$ for the coated sphere. Figure 3(a) gives the normalized effective bulk modulus $\kappa_{\mathrm{eff}}/\kappa_3$ of the coated-sphere assemblage evaluated with Eq. (3) as a function of ratio r_2/r_1. From Fig. 3(a), the acoustic transparency is expected at about $r_2/r_1 = 1.91$, for which $\kappa_{\mathrm{eff}}/\kappa_3 \approx 1$. With the help of Eq. (1), the normalized total-scattering cross sections for the coated sphere (the solid line) and effective single sphere (the dashed line) with κ_{eff}, ρ_3, and r_2 as a function of ratio r_2/r_1 are illustrated in Fig. 3(b). In Fig. 3(b), we can observe a dramatic reduction of the total-scattering cross section of the effective sphere at $r_2/r_1 = 1.91$, as predicted. For the coated sphere, the "position" of the minimum scattering has been shifted upwards due to the large particle effect, analogous to the EM case [1]. The contributions from the first three scattering coefficients of the coated sphere are illustrated in Fig. 3(c). It can be seen that the transparency is largely controlled by the zeroth-order scattering effect. When the particle size is small, the contributions of the higher-order scattering are much smaller compared to the zero-order scattering.

The same computations can be applied for the equal-modulus case, as shown in Fig. 4. The parameters of the coated sphere are $\rho_1 = -0.8\rho_3$, $\rho_2 = 2.5\rho_3$, $\kappa_1 = \kappa_2 = \kappa_3$, and $r_1 = \lambda_3/20$. The normalized effective density $\rho_{\mathrm{eff}}/\rho_3$ of a coated-sphere assemblage calculated with Eq. (6) is shown in Fig. 4(a). According to the method described previously, the acoustic transparency will take place approximately at $r_2/r_1 = 2.22$, for which $\rho_{\mathrm{eff}}/\rho_3 \approx 1$. It is found indeed from the full-wave analyses that the total-scattering cross sections for both the coated sphere (the solid line) and a effective single sphere (the dashed line) are almost zero, as shown in Fig. 4(b). In addition, a resonance phenomenon is observed due to the vanishing denominator of a_1. For a single sphere (ρ, κ_0) embedded in a matrix (ρ_0, κ_0), we examine its first-order scattering coefficient a_1 in the small-particle approximation and find that the resonance will occur when the condition $\rho = -\rho_0/2$ is satisfied. With help of the neutral-
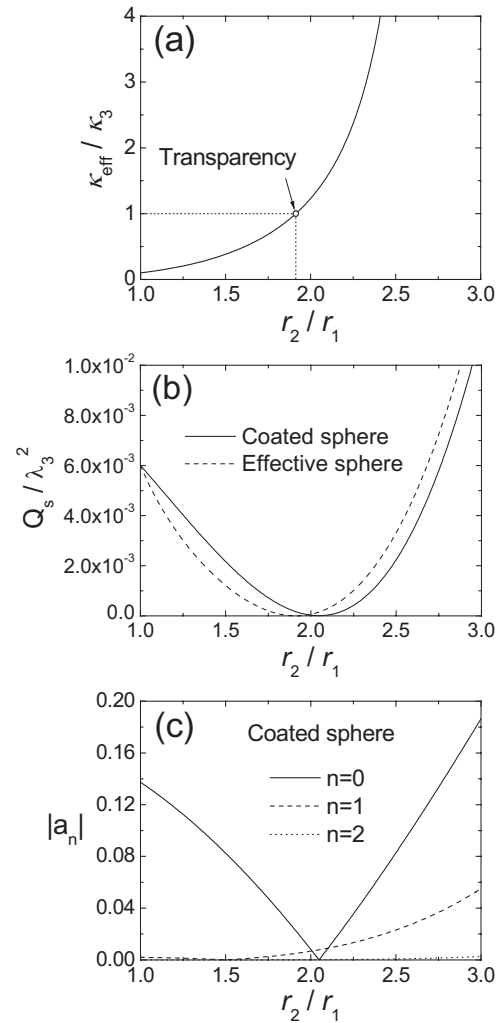

FIG. 3. (a) Normalized effective bulk modulus $\kappa_{\mathrm{eff}}/\kappa_3$ of a coated-sphere assemblage calculated with Eq. (3), (b) normalized total-scattering cross section of a coated sphere (the solid line) and effective homogeneous sphere (the dashed line) with bulk modulus κ_{eff}, density ρ_3, and radius r_2, and (c) contributions of the first three scattering coefficients of the coated sphere vs the ratio r_2/r_1 ($\kappa_1 = 0.1\kappa_3$, $\kappa_2 = -2\kappa_3$, $\rho_1 = \rho_2 = \rho_3$, and $r_1 = \lambda_3/20$).

inclusion concept, the resonance of a coated sphere will take place at the condition $\rho_{\mathrm{eff}} = -\rho_3/2$. Comparing Fig. 4(a) with Fig. 4(b), we can find that the resonance phenomenon is well predicted by $\rho_{\mathrm{eff}}/\rho_3 = -0.5$. The resonance and transparency phenomena due to the first-order scattering effect can be verified in Fig. 4(c), which gives the contributions of the first three scattering coefficients of the coated sphere. It can be found that the first-order scattering effect dominates in this case and other scattering coefficients are small compared to a_1.

Now we discuss the general case by considering the parameters $\kappa_1 = 0.1\kappa_3$, $\rho_1 = -0.2\rho_3$, $\kappa_2 = -2\kappa_3$, $\rho_2 = 1.8\rho_3$, and $r_1 = \lambda_3/20$ for a coated sphere. The effective bulk modulus κ_{eff} and effective density ρ_{eff} of a coated-sphere assemblage calculated with Eqs. (3) and (6), respectively, as a function of ratio r_2/r_1 are shown in Fig. 5(a). Figure 5(b) shows the normalized total-scattering cross sections of the coated sphere (the solid line) and effective single sphere (the dashed
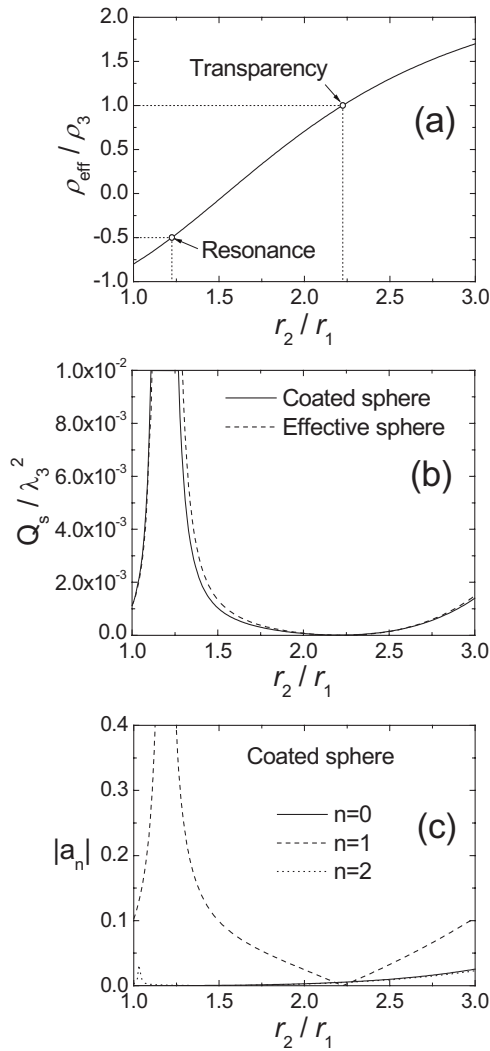
FIG. 4. (a) Normalized effective density ρ_{eff}/ρ_3 of a coated-sphere assemblage calculated with Eq. (6), (b) normalized total-scattering cross section of a coated sphere (the solid line) and effective homogeneous sphere (the dashed line) with bulk modulus κ_3, density ρ_{eff}, and radius r_2, and (c) contributions of the first three scattering coefficients of the coated sphere vs the ratio r_2/r_1 ($\kappa_1 = \kappa_2 = \kappa_3$, $\rho_1 = -0.8\rho_3$, $\rho_2 = 2.5\rho_3$, and $r_1 = \lambda_3/20$).

line) with the bulk modulus κ_{eff} and density ρ_{eff} as a function of the ratio r_2/r_1. According to Fig. 5(a), the designed cover radius is approximately $r_2 = 1.91r_1$, for which $\kappa_{\text{eff}}/\kappa_3 \approx 1$ and $\rho_{\text{eff}}/\rho_3 \approx 1$. From Fig. 5(b), we can see that a low total-scattering cross section of the effective sphere at $r_2/r_1 = 1.91$ can be observed, as predicted. However, for the coated sphere, the corresponding "point" has been shifted upwards. The contributions of the first three scattering coefficients of the coated sphere are shown in Fig. 5(c). When the particle size is very small, it can be seen that the first two scattering coefficients contribute to the final scattering and higher-order scattering coefficients can be neglected.

A doubly coated sphere with the parameters $\kappa_1 = 1.5\kappa_4$, $\rho_1 = 2\rho_4$, $\kappa_2 = 0.2\kappa_4$, $\rho_2 = -0.1\rho_4$, $\kappa_3 = -3.5\kappa_4$, $\rho_3 = 2.2\rho_4$, $r_1 = 0.2r_3$, and $r_3 = 0.1\lambda_4$ is examined in the following. Figure 6(a) gives the effective bulk modulus κ_{eff} and effective density ρ_{eff} of a doubly-coated-sphere assemblage calculated
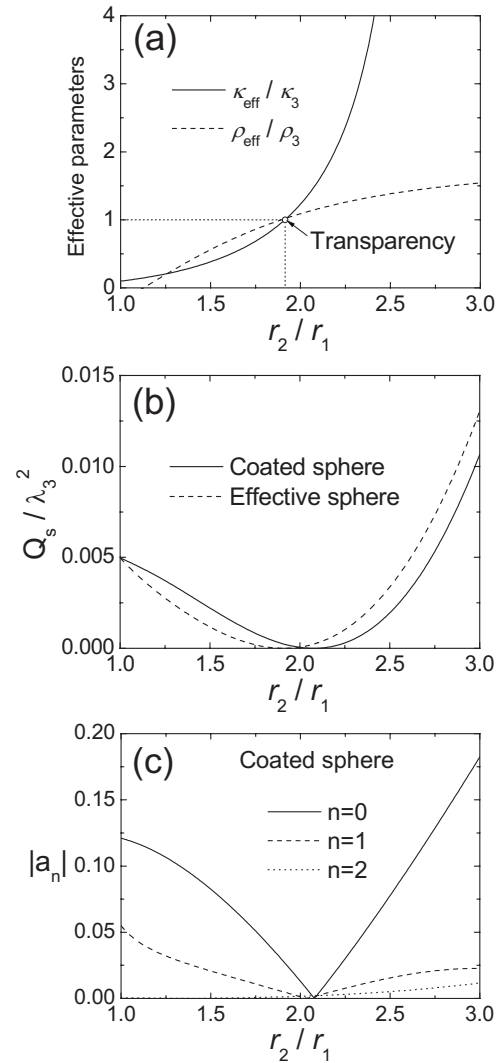
FIG. 5. (a) Normalized effective bulk modulus $\kappa_{\text{eff}}/\kappa_3$ and effective density ρ_{eff}/ρ_3 of a coated-sphere assemblage calculated with Eqs. (3) and (6), respectively, (b) normalized total-scattering cross section of a coated sphere (the solid line) and effective homogeneous sphere (the dashed line) with bulk modulus κ_{eff}, density ρ_{eff}, and radius r_2, and (c) contributions of the first three scattering coefficients of the coated sphere vs the ratio r_2/r_1 ($\kappa_1 = 0.1\kappa_3$, $\rho_1 = -0.2\rho_3$, $\kappa_2 = -2\kappa_3$, $\rho_2 = 1.8\rho_3$, and $r_1 = \lambda_3/20$).

with Eqs. (5) and (8), respectively, as a function of the ratio r_2/r_3. The normalized total-scattering cross sections of the doubly coated sphere (the solid line) and effective single sphere (the dashed line) with the bulk modulus κ_{eff}, density ρ_{eff}, and radius r_3 as a function of ratio r_2/r_3 are shown in Fig. 6(b). The acoustic transparency of the doubly coated sphere is designed approximately at the ratio $r_2/r_3 = 0.63$, for which $\kappa_{\text{eff}}/\kappa_3 \approx 1$ and $\rho_{\text{eff}}/\rho_3 \approx 1$. This can be checked by the result of the effective single sphere shown in Fig. 6(b), where a low total-scattering cross section at around the ratio $r_2/r_3 = 0.63$ can be observed, while for the doubly coated sphere, the corresponding "point" has been shifted downwards, due to the large particle effect.

Realization of acoustic transparency can be further checked when we examine the contour plot of scattered
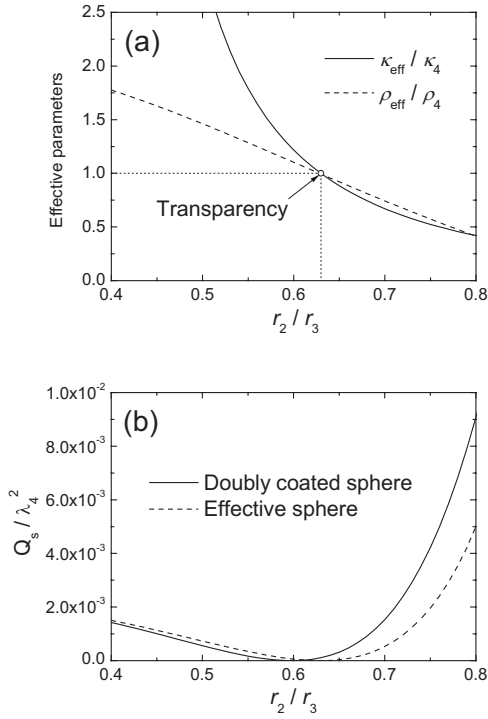
FIG. 6. (a) Normalized effective bulk modulus $\kappa_{\mathrm{eff}}/\kappa_3$ and effective density $\rho_{\mathrm{eff}}/\rho_3$ of a doubly-coated-sphere assemblage calculated with Eqs. (5) and (8), respectively, and (b) normalized total-scattering cross sections of a doubly coated sphere (the solid line) and effective homogeneous sphere (the dashed line) with bulk modulus κ_{eff}, density ρ_{eff}, and radius r_3 vs the ratio r_2/r_3 ($\kappa_1 = 1.5\kappa_4$, $\rho_1 = 2\rho_4$, $\kappa_2 = 0.2\kappa_4$, $\rho_2 = -0.1\rho_4$, $\kappa_3 = -3.5\kappa_4$, $\rho_3 = 2.2\rho_4$, $r_1 = 0.2r_3$, and $r_3 = 0.1\lambda_4$).

fields excited by a coated sphere. For comparison, we first examine a single sphere with parameters $\kappa_1 = 0.1\kappa_3$, $\rho_1 = -0.2\rho_3$, and $r_1 = \lambda_3/20$ incident by a plane compressional wave along the z direction, as shown in Fig. 7(a). The magnitude of the radial component of the displacement field of the scattered wave in the x-z plane is plotted in Fig. 7(c). It is clearly seen that the single sphere generates the scattered fields outside of the sphere. When a coating with parameters $\kappa_2 = -2\kappa_3$, $\rho_2 = 1.8\rho_3$, and $r_2 = 2.1r_1$ is employed, as shown in Fig. 7(b), the contour plot of the scattered fields of the coated sphere is shown in Fig. 7(d). It can be seen in Fig. 7(d) that the cover almost cancels the scattered radiation outside. For this case, the coated sphere has a very small total-scattering cross section. The effect of the cover is very similar to that of the plasmonic coating for the EM wave transparency [1].

From all the analyses given above, it is evident that the acoustic-wave transparency of a multilayered sphere can be realized, for which the total-scattering cross section is dramatically reduced. The transparency and resonance phenomena in the full-wave computations can be well predicted by the quasistatic conditions, obtained with the neutral-inclusion concept.

It is known that complete transparency will be achieved when the total-scattering cross section of a particle is zero. However, from the above computations, it is found that the total-scattering cross section can be extremely low, but never be zero. So it is necessary to discuss the distribution of the
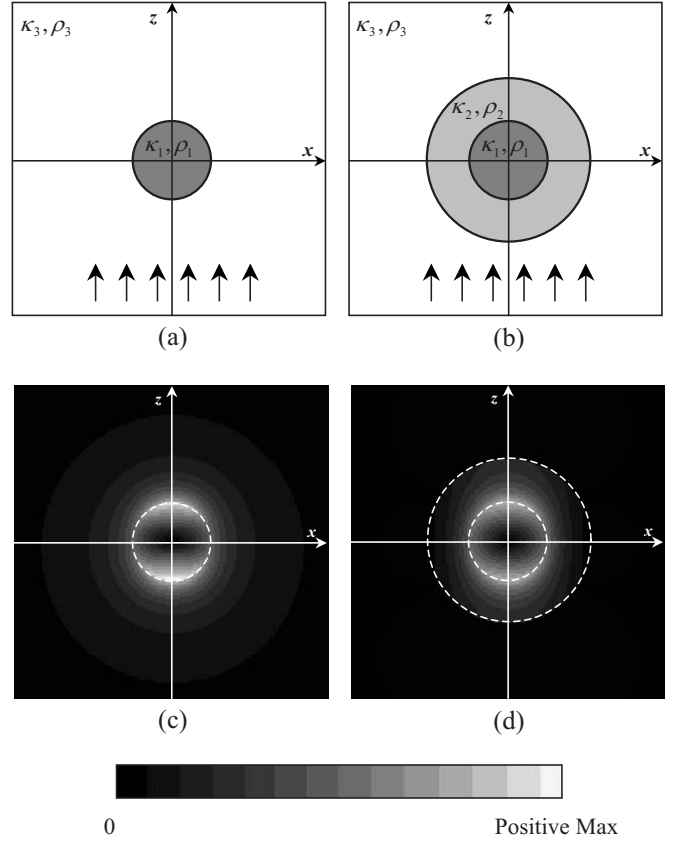

FIG. 7. The schemes of (a) a single sphere with $\kappa_1 = 0.1\kappa_3$, $\rho_1 = -0.2\rho_3$, and $r_1 = \lambda_3/20$ and (b) the same sphere covered with $\kappa_2 = -2\kappa_3$, $\rho_2 = 1.8\rho_3$, and $r_2 = 2.1r_1$, incident by a plane compressional wave along the z direction as well as the contour plots of the distribution of radial component of the scattered displacement field in the x-z plane for (c) the single sphere and (d) coated sphere.

scattered field in space. After reflection and refraction by a particle, the incident wave may be localized in some particular directions. The angle distribution of the scattered acoustic wave in space can be evaluated by the differential scattering cross section σ_d, which is calculated by [18]

$$\sigma_d(\theta) = \lambda_{L+1}^2 \left| \sum_{n=0}^{\infty} (-i)^{n+1} a_n P_n(\cos\theta) \right|^2 \Big/ (4\pi^2), \quad (10)$$

where P_n is the Legendre function. Using the same parameters as in Fig. 3, we compute the angle-dependent differential scattering cross sections of coated spheres with different cover radii $r_2 = 2r_1$, $r_2 = 2.05r_1$, and $r_2 = 2.1r_1$, as shown in Fig. 8. For the purpose of macroscopic transparency (lower total-scattering cross section), the coated sphere is best with the cover radius $r_2 = 2.05r_1$, compared to those with $r_2 = 2r_1$ and $r_2 = 2.1r_1$. However, this configuration is not the best if we examine the scattering from other directions; for example, it has larger scattering cross sections in the forward direction compared to the coated sphere with $r_2 = 2r_1$ and in the backward direction compared to that with $r_2 = 2.1r_1$. For further study, we can calculate the backscattering or sonar $[\sigma_b = 4\pi\sigma_d(\pi)]$ and forward $[\sigma_f = 4\pi\sigma_d(0)]$ scattering cross sections of the coated sphere as a function of ratio r_2/r_1. The
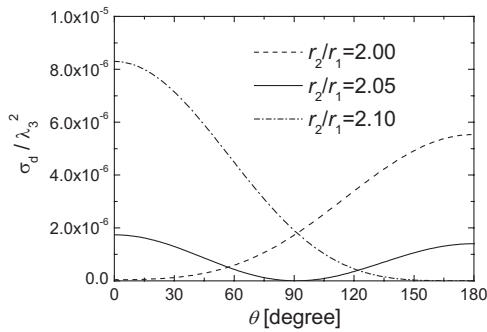
FIG. 8. The angle-dependent normalized differential scattering cross section of a coated sphere for three different cover radii r_2 $=2r_1$, $r_2=2.05r_1$, and $r_2=2.1r_1$ ($\kappa_1=0.1\kappa_3$, $\kappa_2=-2\kappa_3$, $\rho_1=\rho_2=\rho_3$, and $r_1=\lambda_3/20$).

results are shown in Fig. 9, where the total-scattering cross section [which has been plotted as the solid line in Fig. 3(b)] is plotted again for comparison. It is observed that the transparency phenomena resulting from the three scattering cross sections are not realized in the same configuration. These results show that the scattering over all directions is not equally reduced when we lower the total scattering cross section. So if we would like to improve the transparency, the scattering from all directions must also be minimized simultaneously. This kind of problem may be solved when an anisotropic metamaterial [2,3] is introduced.

In this paper, we investigate composite spheres that are made of fluidlike materials to achieve acoustic transparency. A simple configuration to realize the transparency may be composed of a fluid acoustic metamaterial covered by a soft rubber. When a concentric shell made of fluids is concerned, the manufacturing of multilayered spheres seems to be challenging. However, we can let the fluid shell be sandwiched by soft rubber to construct a multilayered system. Then the parameters of the whole system can be determined with the help of the transparency condition of a multilayered sphere. It is also expected that acoustic metamaterials with a solid nature can be designed and fabricated in the future. In that case, the manufacturing of multilayered spheres can be rela-
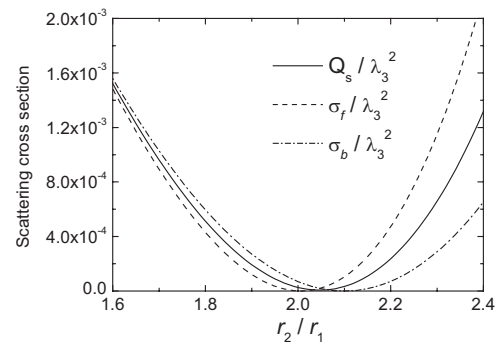

FIG. 9. The normalized backscattering (σ_b), forward-scattering (σ_f), and total-scattering cross sections (Q_s) of the coated sphere as a function of the ratio r_2/r_1 ($\kappa_1=0.1\kappa_3$, $\kappa_2=-2\kappa_3$, $\rho_1=\rho_2=\rho_3$, and $r_1=\lambda_3/20$).

tively easy. However, the influences of shear waves localized in the composite structure on the transparency must be evaluated. The relevant analyses will be given in our future work.

IV. SUMMARY

To conclude, we have investigated the acoustic transparency phenomenon induced by metamaterials. With help of the neutral-inclusion concept, the quasistatic transparency conditions are derived for a multilayered sphere in three cases—i.e., equal-density, equal-modulus, and general cases. Numerical results by full-wave analyses have been conducted to verify these quasistatic conditions. It is also found that, to improve the transparency, the scattering of particles in all directions must also be reduced. Finally, we indicate that objects other than multilayered spheres can be easily designed to be acoustically transparent with the neutral-inclusion concept.

[1] A. Alù and N. Engheta, Phys. Rev. E **72**, 016623 (2005).

[2] J. B. Pendry, D. Schurig, and D. R. Smith, Science **312**, 1780 (2006).

[3] U. Leonhardt, Science **312**, 1777 (2006).

[4] A. Hendi, J. Henn, and U. Leonhardt, Phys. Rev. Lett. **97**, 073902 (2006).

[5] X. M. Zhou and G. K. Hu, Phys. Rev. E **74**, 026607 (2006).

[6] D. R. Smith, J. B. Pendry, and M. C. K. Wiltshire, Science **305**, 788 (2004).

[7] D. Schurig, J. J. Mock, B. J. Justice, S. A. Cummer, J. B. Pendry, A. F. Starr, and D. R. Smith, Science **314**, 977 (2006).

[8] V. G. Veselago, Sov. Phys. Usp. **10**, 509 (1968).

[9] J. Li and C. T. Chan, Phys. Rev. E **70**, 055602(R) (2004).

[10] S. Yang, J. H. Page, Z. Liu, M. L. Cowan, C. T. Chan, and P. Sheng, Phys. Rev. Lett. **93**, 024301 (2004); X. D. Zhang and Z. Y. Liu, Appl. Phys. Lett. **85**, 341 (2004).

[11] S. Foteinopoulou, E. N. Economou, and C. M. Soukoulis, Phys. Rev. Lett. **90**, 107402 (2003); E. Cubukcu, K. Aydin, E. Ozbay, S. Foteinopoulou, and C. M. Soukoulis, Nature (London) **423**, 604 (2003).

[12] R. S. Lakes, Phys. Rev. Lett. **86**, 2897 (2001).

[13] N. Fang, D. Xi, J. Xu, M. Ambati, W. Srituravanich, C. Sun, and X. Zhang, Nat. Mater. **5**, 452 (2006).

[14] G. W. Milton, *The Theory of Composites* (Cambridge University Press, Cambridge, England, 2002), pp. 113–142.

[15] C. F. Ying and R. Truell, J. Appl. Phys. **27**, 1086 (1956).

[16] Z. Hashin and S. Shtrikman, J. Mech. Phys. Solids **11**, 127 (1963).

[17] J. G. Berryman, J. Acoust. Soc. Am. **68**, 1809 (1980).

[18] N. B. Kakogiannos and J. A. Roumeliotis, J. Acoust. Soc. Am. **98**, 3508 (1995).